Journal of Coastal Conservation (2025) 29:91
https://doi.org/10.1007/s11852-025-01160-8

Geospatial modelling for sinkhole hazard in the coastal area of Safi, Morocco

Fatima El Bchari[1] · Jorge Trindade[2,4,5] · Abdessamad Charif[3] · Mohamed Chaibi[3] · Abdellah Khouz[4,6] · Halima Ait Malek[1]

Received: 14 February 2023 / Revised: 18 January 2024 / Accepted: 3 October 2025
© The Author(s), under exclusive licence to Springer Nature B.V. 2025

Abstract
Collapse sinkholes represent a geological hazard that is particularly associated with karst regions, characterized by the dissolution of soluble rocks leading to the formation of voids. This phenomenon is significantly more prevalent in areas with evaporate terrains, wherein the rapid dissolution of soluble rocks facilitates the swift alteration of gap locations and sizes. The ensuing discussion explores the distinctive nature of collapse sinkholes, emphasizing their occurrence in karst and evaporate terrains, shedding light on the factors contributing to their formation and frequency. The coastal region of Safi is characterized by abundant karst features overlying evaporitic rocks, along with historical and recent sinkhole collapse events. Our current investigation aims to develop a susceptibility map for sinkhole collapse in the Safi region. Initially, a comprehensive inventory map of collapse occurrences was created through meticulous fieldwork and the integration of remote sensing data. Nine predisposing factors were identified and incorporated into a Geographic Information System (GIS), including elevation, lithology, curvature, slope, aspect, drainage density, lineament density, topographic wetness index, and land use. To assess the relationship between these factors and sinkhole collapse, statistical analyses were conducted using spatial analysis based on the Frequency Ratio (FR) and Analytical Hierarchy Process (AHP). The FR analysis revealed that high and very high susceptibility zones constitute 14.19% and 6.89% of the region, respectively, while moderate, low, and very low susceptibility zones occupy 23.07%, 26.12%, and 29.74%, respectively. Utilizing the AHP method, it was determined that high and very high susceptibility zones cover 20.32% and 12.01% of the region, respectively, with moderate, low, and very low susceptibility zones encompassing 19.38%, 27.55%, and 20.74%, respectively. To compare and evaluate the outcomes of the AHP and FR methods, the Area Under the Curve (AUC) approach was employed. The success rates, as indicated by AUC, demonstrated that FR (90.5%) exhibited higher accuracy than AHP (73.5%). The validation of the landslide susceptibility map confirmed the acceptability of the methodologies employed. These results can be effectively utilized for hazard mitigation and land use planning in the coastal area of Safi.

Keywords Sinkholes; controlling factors · AHP · FR · Susceptibility · Morocco. GIS · AUC

✉ Fatima El Bchari
elbchari@uca.ac.ma

[1] Department of Earth Sciences, GEGEL Group, Cadi Ayyad University, Polydisciplinary Faculty, Safi, Morocco

[2] Department of Sciences and Technology, University of Aberta, Lisbon, Portugal

[3] Department of Geograpghy, GEGEL Group, Polydisciplinary Faculty, Safi, Morocco

[4] Centre of Geographical Studies, University of Lisboa, Lisbon, Portugal

[5] Centre for Functional Ecology - Science for People & the Planet, Coimbra University, Coimbra, Portugal

[6] Centro de Estudos Globais, Aberta University, Lisbon, Portugal

Introduction

Karst landscapes are characterized by distinctive surface and subsurface hydrology and geomorphology resulting from the dissolution of limestones and/or evaporitic rocks (Ford and Williams 2007). This process, known as karstification, serves as a precursor for the development of underground cavities of varying sizes (Weisrock and Lunski 1987; Gutiérrez et al. 2007; Parise 2010; Kaufmann 2014). Karst systems encompass a variety of features such as subsurface drainage, the absence of a surface drainage network, shallow or deep sinkholes, poljes, springs, and high permeability aquifers with conduits and caves. Of these, sinkholes

Published online: 09 December 2025

are particularly significant for diagnostic purposes (Ford and Williams 2007), and for this research, the term "sinkhole" is adopted to denote the morphological evidence of the aforementioned processes.

Sinkholes typically exhibit subcircular shapes and various morphological characteristics such as conical, pan-shaped, bowl-shaped, and cylindrical, often extending deep for hundreds of meters in diameter and depth (Renault 1970). Recent research classifies sinkholes into categories including ground surface corrosion, sagging, suffusion, and collapse (Gutiérrez et al. 2014; Gutiérrez et al., 2008a, Gutiérrez et al. 2008b, Gutiérrez et al. 2008c, d, Gutiérrez et al. 2009; Waltham et al. 2005; Paine et al. 2012). These processes are associated with karst rocks, wherein dissolution leads to the formation of "solution dolines" resembling bowl-shaped depressions. Sagging occurs due to continuous flexing of overlaying carboniferous units during dissolution, while corrosion between the topsoil and substratum creates depressions on the surface, and interlayer dissolution may cause the limestone to bend.

Sinkhole formation is initiated by the collapse of cavity roofs, rocks, and soil. Cohesive rock/soil results in "cover collapse dolines," while non-cohesive soil gives rise to "suffusion dolines." Consequently, sinkholes represent a form of land movement associated with the presence of underground cavities, developing through a prolonged process of karstification. The resultant damage from sinkholes can have severe consequences, affecting various infrastructures such as roads, railroads, power lines, and may even lead to loss of life.

The hazards posed by karst environments and their local and regional socio-economic impacts have escalated rapidly with urban sprawl and development, often lacking appropriate land use planning measures that consider the specificity of these environments (Goudie 2013; Gutiérrez et al., 2014). Assessing susceptibility to sinkhole collapse involves determining the spatial probability of ground collapse (Guzzetti et al. 1999; Constantin et al. 2011). This information is crucial for effective land use management and planning (Galve et al. 2009; Taheri et al. 2019; Dai et al. 2008). The accuracy of sinkhole susceptibility mapping depends on data availability, spatial distribution of sinkholes, and the selection of relevant conditioning and triggering factors and modeling approaches.

Various methods, both qualitative and quantitative, are employed for mapping sinkhole susceptibility. Quantitative modeling, including deterministic and probabilistic approaches, is commonly used (Zhou and Beck 2008; Galve et al. 2009; Praveen et al. 2019). Deterministic approaches consider variables affecting sinkhole formation based on geometric assumptions, while probabilistic methods assume statistical relationships between predisposing factors and known sinkhole locations (Galve et al. 2009; Whitman et al., 1999; Ciotoli et al. 2016).

Alternatively, qualitative or heuristic approaches involve subjective grading schemes based on factor contributions to sinkhole development (Gao and Alexander 2003; Taheri et al. 2020). Hybrid (or semi-heuristic) approaches, like weighted linear combination, can also be employed for creating susceptibility maps (Yalcin 2008; Yalcin et al. 2011, Park et al. 2012). The Analytic Hierarchy Process (AHP) is a statistical approach for susceptibility mapping that involves decomposing controlling factors into subclasses, hierarchical arrangement, pairwise comparisons, and synthesis to obtain susceptibility metrics (Yalcin 2008; Komac 2006; Praveen et al. 2019; Ozdemir 2015; Khouz et al. 2022).

Weisrock and Lunski (1987), Ouadia et al. (2008), Theilen-Willige et al. (2014), and Laaziz et al. (2016) have studied sinkhole morfologies in the Safi region of Morocco. While these studies presented GIS-based thematic maps, none of them focus on predictive models for sinkhole susceptibility. This research introduces sinkhole susceptibility assessment in the coastal area of Safi, employing both the Analytical Hierarchy Process (AHP) and the Frequency Ratio (FR) approach.

The main objective of sinkhole susceptibility mapping is to assess and predict the occurrence of sinkholes in a given geographical area. This complex process integrates a range of geological, hydrological and geomorphological factors to generate accurate susceptibility maps. The mapping effort is designed to highlight the areas most prone to sinkhole collapse, providing crucial information for activities such as hazard mitigation, land-use planning and risk management in regions vulnerable to this type of geological event. Ultimately, the aim is to advance our understanding of sinkhole dynamics and contribute to informed decisions about land use and development in sinkhole-prone areas.

Presentation of the study area

The Safi Province, part of the Marrakech-Safi region, covers an area of 3633 km with a coastal length exceeding 120 km. It is bordered to the north by the Sidi Bennour province, to the east by Youssoufia, to the south by the Essaouira province, and to the west by the Atlantic coast (Fig. 1).

Geographically, Safi is located at 32° 19' North and 9° West. The province's terrain is characterized by a relatively flat or gently undulating topography, with elevations seldom exceeding 500 m above sea level.

From a geomorphological perspective, the area of investigation is divided into three zones.

– Sahel: Including consolidated Pliocene and Quaternary dunes and dune ridges forming the current shoreline. These formations are composed of encrusted limestone

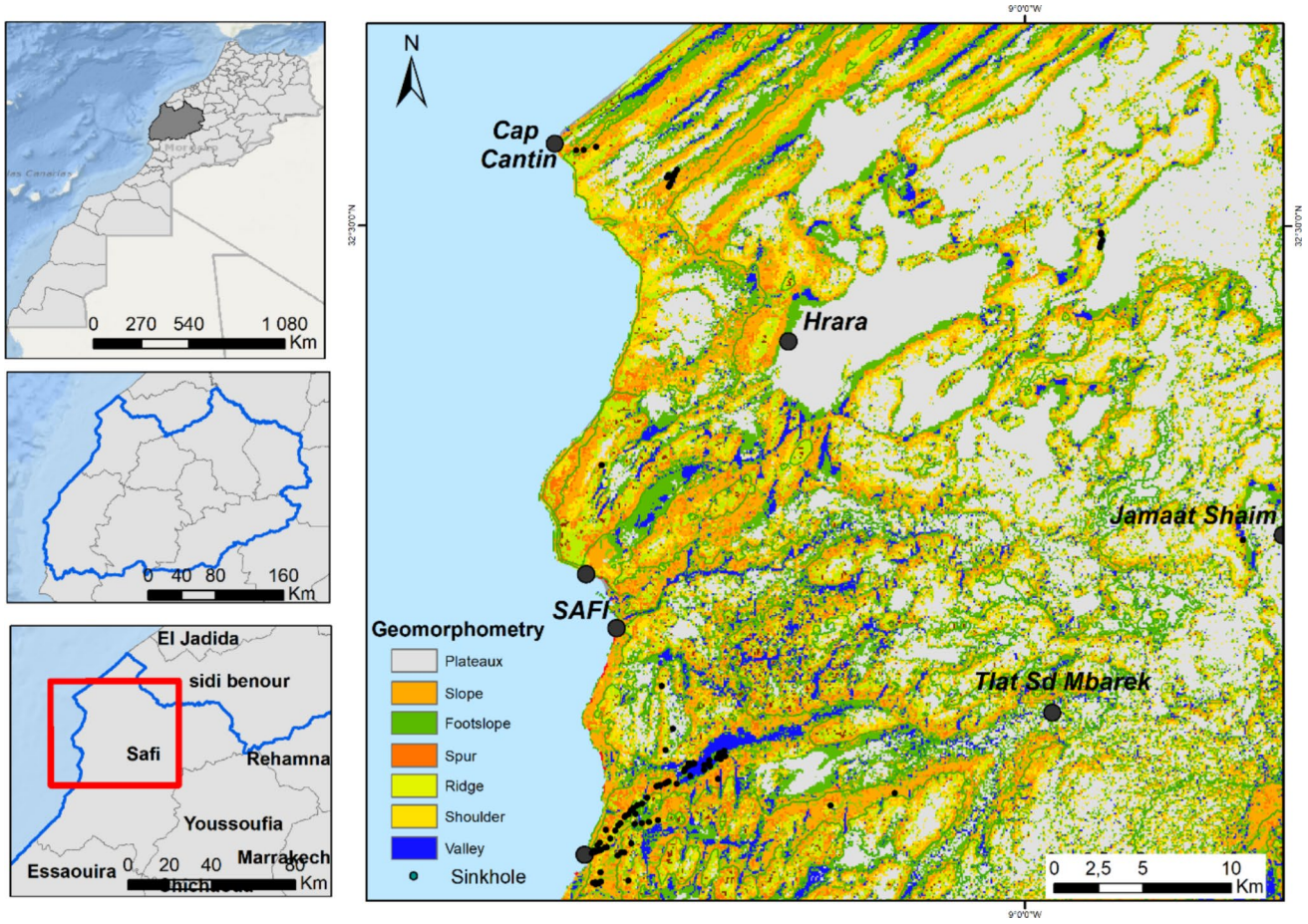

Fig. 1 Location and geomorphometric map of the study area

sandstones, with the subsurface often composed of Jurassic limestone and occasionally gypsum outcrops to the east of Safi.

– Plain: a natural southward extension of the Doukkala plain. It is a collection of gentle slopes starting behind the Sahel and connecting to the Mouissates hills. The plain's lithology primarily consists of recent Quaternary silts that form corridors between consolidated hills.
– Mouissates Hills: Dominating the western and eastern parts of the Abda plain, these hills connect to the plain through rugged slopes. Inside the Mouissates, the landscape appears as a plateau dissected by an ancient deep hydrographic network, defining steep slopes. This geomorphological unit is composed of gypsum and limestone of Upper Jurassic and terminates to the south with Jbel Hadid, crossed by the Tensift River.

According to the latest administrative division, the Safi province comprises 3 municipalities and and three rural circles with 22 rural communes. According to the General Population and Housing Census of 2014, the population of Safi province was 691,983 inhabitants, representing 15.4% of the Marrakech-Safi region's population and 2% of the national population. It recorded an average annual growth rate of 0.73% compared to 2004. The provincial urbanization rate in 2014 was 50%, compared to 42.8% regionally and 60.4% nationally.

The study area is situated in the western Meseta region of Morocco, characterized by a Meso-Cenozoic tabular sediment cover overlying a Paleozoic substratum (Fig. 1) (Roch 1950; Gigout 1951; Michard 1976; Witam 1988). Overall, the topography of the study area is predominantly flat, with the altitude gradually decreasing from 480 to 0 m towards the West.

The stratigraphic series in the Safi area is composed of distinct units arranged from Upper Jurassic to Quaternary, (Fig. 2 and 3). The following is an overview of the geological composition of the Safi region: (a) Upper Jurassic limestones with gypsum, (b) The lower Cretaceous (Late Berriasian – Valanginian) bioclastic limestone (C1), (c) The "brown clay" (Ci2a) of Valanginian—lower Hauterivian, characterized by grey marl with marly limestones, (d) Cretaceous (Upper Hauterivian) limestones and sandstone of Dridrat (Ci2b), exhibiting various karstification shapes, (e)

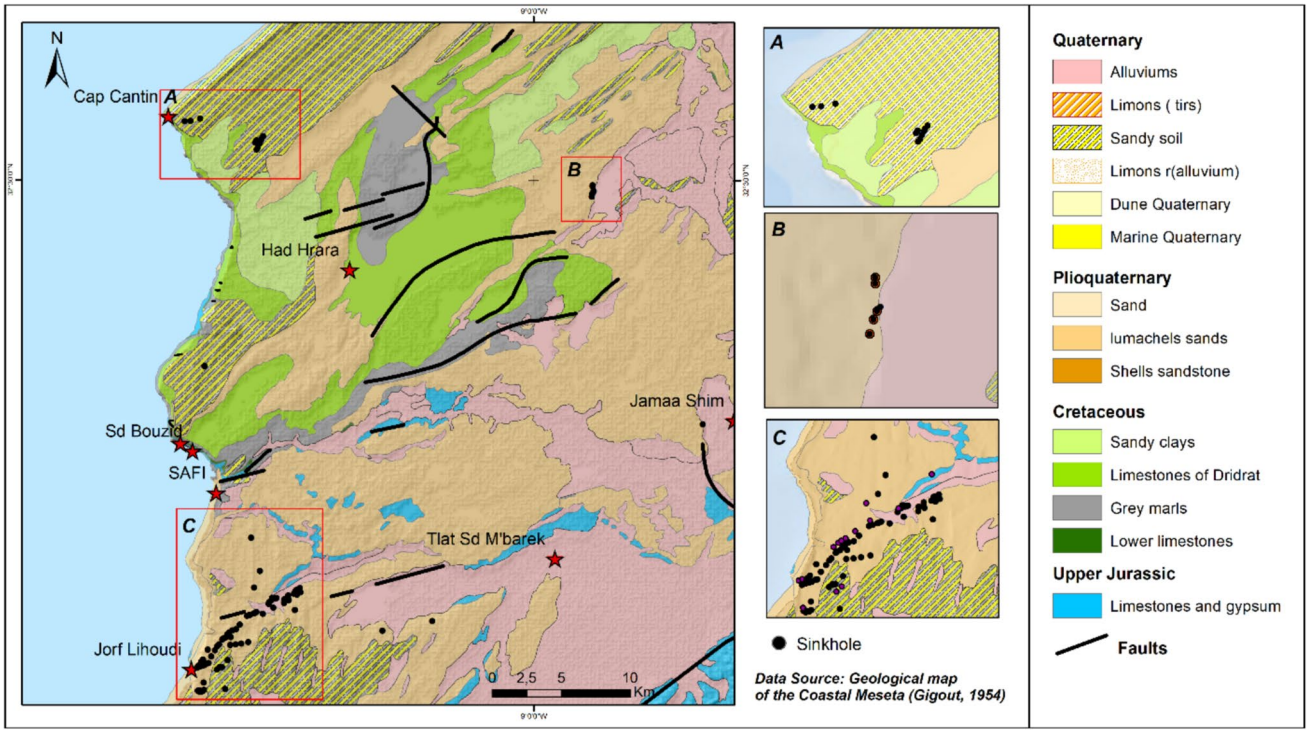

Fig. 2 Geologic map of the study area (adapted from Gigout, 1954)

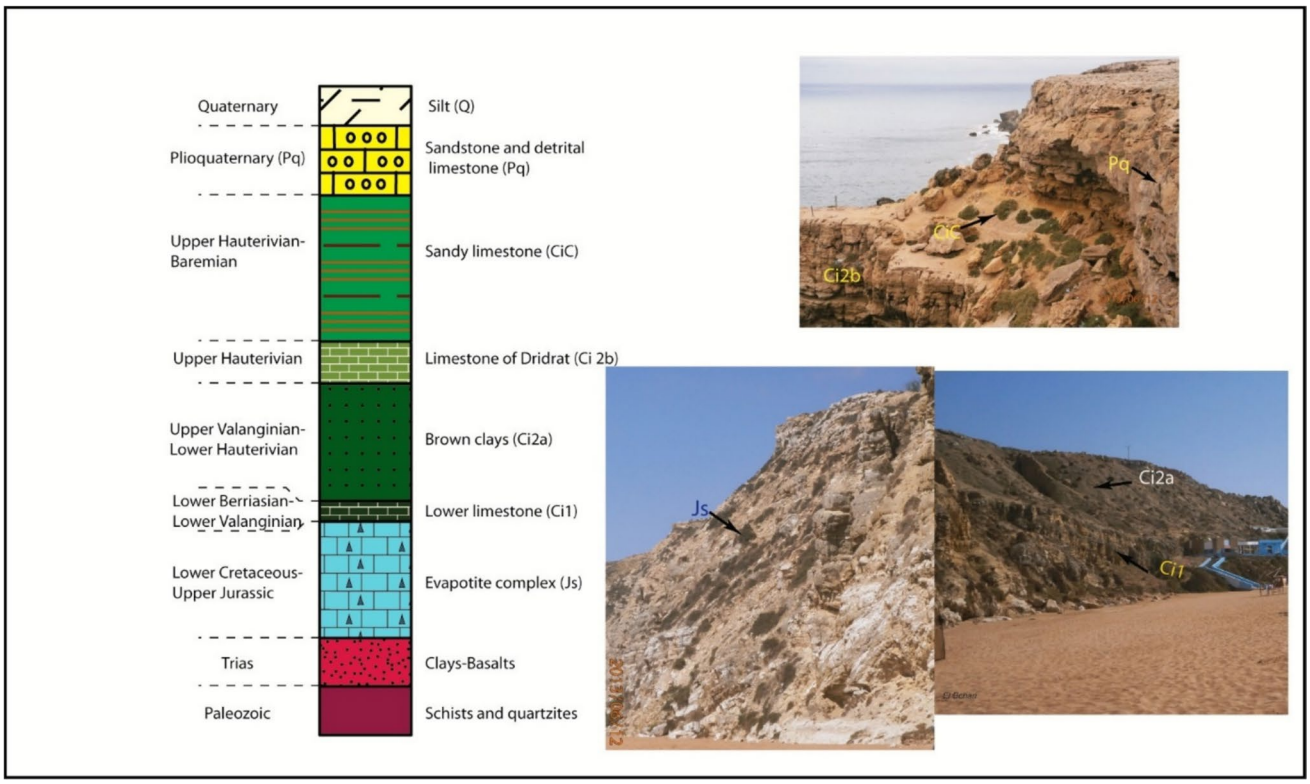

Fig. 3 Stratigraphic log of the study area

The "red sandy clay beds" of the Upper Hauterivian (Cic), along with bioclastic limestone of Pliocene and consolidated dune of Plioquaternary.

The structural framework is primarily of tertiary origin and can be defined by two major fold orientations, namely N-S and SW-NE to E-W, which are linked respectively to the Hercynian and Alpine orogenies (Ferré and Ruhard 1975).

The aquifer systems in the Safi region are mainly comprised of the Dridrat Limestone from the lower Cretaceous and quaternary sandstone, emphasizing the hydrogeological significance of these formations in the region. Overall, the geological complexity of the Safi region contributes to its diverse landscape and environmental characteristics.

The Safi region is characterized by a semi-arid climate, featuring distinct climatic patterns throughout the year. The climate in Safi characterized by hot and dry summers lasting from May to November, followed by a wet and temperate winter period from November to April.

The semi-arid climate of Safi reflects the influence of its geographic location and topography. While the summers are marked by arid conditions and high temperatures, the winter months bring relief with cooler temperatures and a higher likelihood of precipitation.

Analysing the rainfall data from 1960 to 2021, the average annual precipitation in Safi is approximately 354 mm. The minimum recorded rainfall occurred in 1981, measuring 146 mm, while the maximum was observed in 1996, reaching 712 mm. These fluctuations in precipitation contribute to prolonged droughts as well as sudden and intense rainfall, which can lead to local flash floods.

The wettest month in Safi is January, with an average rainfall of 35 mm. The mean annual temperature in the area is 24 °C, with July being the warmest month, boasting an average temperature of 31°C. Conversely, January is typically the coldest month in Safi, with an average temperature of 18°C.

Methodology

The methodology employed for sinkhole susceptibility mapping is a systematic and comprehensive approach designed to assess and predict the likelihood of sinkhole occurrence in a given geographic area. This multifaceted process integrates various techniques and steps to derive a reliable and accurate sinkhole susceptibility map.

It begins with the collection of pertinent geological, hydrological, and geomorphological data through field surveys, remote sensing technologies, and historical records. Ensuring the quality and consistency of acquired data is paramount, involving cleaning and preprocessing to create a standardized format suitable for subsequent analysis.

The identification of predisposing factors influencing sinkhole formation is crucial, with variables such as lithology, slope, land use, drainage density, and elevation selected based on their relevance. The choice of an appropriate modeling method, including Frequency Ratio (FR), Analytical Hierarchy Process (AHP), logistic regression, or machine learning algorithms, is a pivotal decision.

Weighting and ranking factors come next, with techniques like pairwise comparisons in AHP aiding in establishing criteria importance. The chosen model is then applied to spatial data layers, generating individual susceptibility maps for each factor. These maps are overlaid or combined to create a consolidated sinkhole susceptibility map, considering the weighted contribution of each factor.

Validation is a critical step, assessing the accuracy and reliability of the susceptibility map using independent sinkhole data or historical records. Depending on validation results, the model may undergo refinement, adjusting weights or parameters to enhance accuracy. The final sinkhole susceptibility map is presented, highlighting high-risk zones, and interpretation of results is crucial for understanding implications.

For the current study, a comprehensive sinkhole inventory was compiled by using various data sources, including topographical maps, aerial photographs, satellite imagery, borehole data, and extensive fieldwork.

The primary objective was to identify and document key parameters such as location, size, shape, depth, and geological context of the sinkholes. A meticulous examination of 104 sinkhole locations was conducted through fieldwork, with each sinkhole being described, mapped, and validated (Fig. 2 and 4).

Sinkhole susceptibility analysis, contingent on data availability, can incorporate numerous influencing factors such as lithology, fault lineaments, streams, roads, water table, rainfall, slope, aspect, and land use/land cover. In this study, diverse datasets were harnessed, including a digital elevation model (DEM) based on shuttle radar topography mission data, geological maps, topographic maps, Landsat 8 and Sentinel satellite images, and data collected directly in the field (Fig. 5).

The dataset variables encompassed elevation, slope, aspect, curvature, drainage density, lineament density, topographic wetness index (TWI), lithology, and land use/land cover (LU/LC) (Table 1 and Fig. 6). To ensure consistency, all variables were rasterized and harmonized to a cell size of 30 m × 30 m. Drainage density was assessed using the hydrographic network based on topographic maps (1/25000) and the DEM. The DEM also facilitated the determination of slope, aspect, curvature, and elevation, while the TWI was derived from it.

Fig. 4 Example of the sinkhole collapse in the study area

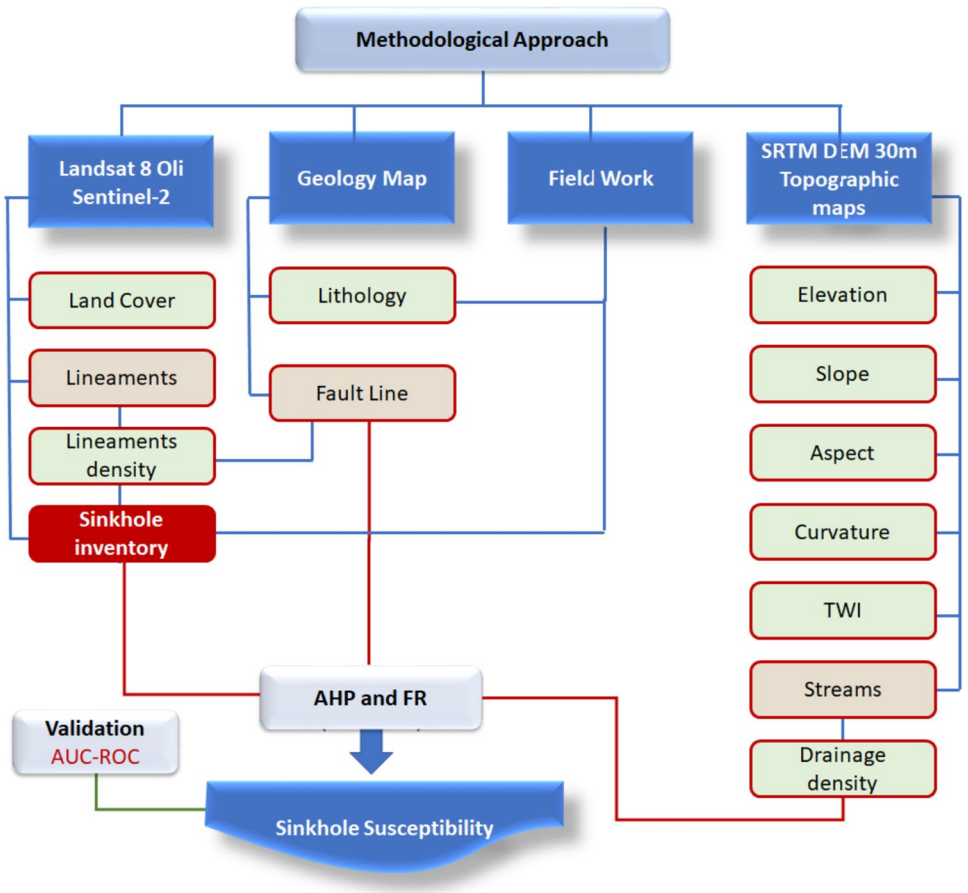

Fig. 5 Methodology adopted for the study

Table 1 Data Sources used for our research

Data	Description	Source
Elevation (m)	extracted from SRTM 30 m	https://earthexplorer.usgs.gov
Slope angle and Slope aspect	extracted from SRTM 30 m	https://earthexplorer.usgs.gov
TWI	extracted SRTM 30 m	https://earthexplorer.usgs.gov
Land use	extracted from Landsat 8 Oli image and field observation	https://earthexplorer.usgs.gov
Lineament	Digitized from geological map of Safi Derived from Landsat 8 and sentinel images	Geological map of Meseta between Machraa Benabbou and Safi 1:200.000 (Gigout, 1954) Landsat 8 and sentinel-2 images
Lineament density	Calculated	
Streams	Digitized and extracted	Topographic maps 1/25000 and SRTM 30 m
Stream density density	Calculated	
Lithology	Digitized from geological map of Safi	Geological map of Meseta between Machraa Benabbou and Safi 1:200.000 (Gigout, 1954)/Field work
Sinkhole location	Digitized and extracted from Landsat 8 and Sentinel-2 images	Field work/topographic maps 1/25000 and Satellite images

Information regarding lithology and faulting was extracted from the 1:200,000 geological map. The fracturation map was generated through image filter processing of a Landsat TM image. Lastly, supervised classification of LANDSAT 8 Oli and Sentinel-2 images was conducted to obtain the distribution of land use/land cover in the study area. This comprehensive and multi-faceted approach ensures a robust foundation for sinkhole susceptibility mapping, integrating fieldwork, remote sensing, and a variety of spatial data sources to enhance accuracy and reliability.

The mapping process involves assessing and predicting the likelihood of sinkhole occurrences by considering the the nine factors listed above. By integrating these factors through sophisticated modeling techniques, we aim to produce accurate susceptibility maps that aid in effective land use management, infrastructure planning, and risk mitigation in vulnerable regions.

In recent years, various methodologies have been employed for sinkhole susceptibility mapping, including frequency ratios, analytical hierarchy processes, bivariate and multivariate analysis, logistic regression, fuzzy logic, and artificial neural networks (Saaty 1977; Dogan & Yilmaz 2011; Aurit et al. 2013; Lamelas et al. 2008).

The selection of the Frequency Ratio (FR) and Analytical Hierarchy Process (AHP) methods for sinkhole susceptibility mapping is justified by their complementary strengths and suitability for achieving the study's objectives. The Frequency Ratio method offers simplicity and computational efficiency, making it ideal for large-scale studies, and establishes a statistical relationship between sinkholes and influencing factors. Its wide applicability in landslide and collapse susceptibility analysis enhances its reliability. On the other hand, the Analytical Hierarchy Process is chosen for its ability to handle complex decision-making involving multiple factors. AHP's hierarchical structure and incorporation of expert judgment through pairwise comparisons facilitate a nuanced understanding of the interplay between various factors. Additionally, the consistency checks in AHP contribute to the robustness of the decision-making process. Together, the combination of FR and AHP aims to provide a comprehensive and accurate sinkhole susceptibility mapping approach, considering both statistical analysis and expert input to address the geological complexity of the study area.

In the context of sinkhole susceptibility mapping of the Safi area, the modeling steps for the Frequency Ratio (FR) method and Analytical Hierarchy Process (AHP) can be outlined. The Frequency Ratio (FR) method involves several key steps. Initially, relevant data, including geological and hydrological factors, are collected and a sinkhole inventory map is prepared. Subsequently, predisposing factors such as lithology, slope, and land use are identified, and weights are assigned based on their impact on sinkhole occurrence. The FR formula is then applied to calculate the susceptibility index for each factor, and these individual maps are overlaid to create a comprehensive sinkhole susceptibility map.

Conversely, the Analytical Hierarchy Process (AHP) method follows a distinct set of steps. A hierarchical structure is first formed, outlining criteria and sub-criteria influencing sinkhole susceptibility. Pairwise comparisons are conducted to establish the relative importance of each criterion and sub-criterion, with a subsequent consistency check. Weights are calculated based on these comparisons, normalized to ensure a sum of 1, and applied to spatial data layers representing each criterion. The weighted layers are then combined to generate the final sinkhole susceptibility map. Similar to the FR method, the AHP model is validated using independent sinkhole data or historical records to ensure its reliability and applicability to real-world conditions.

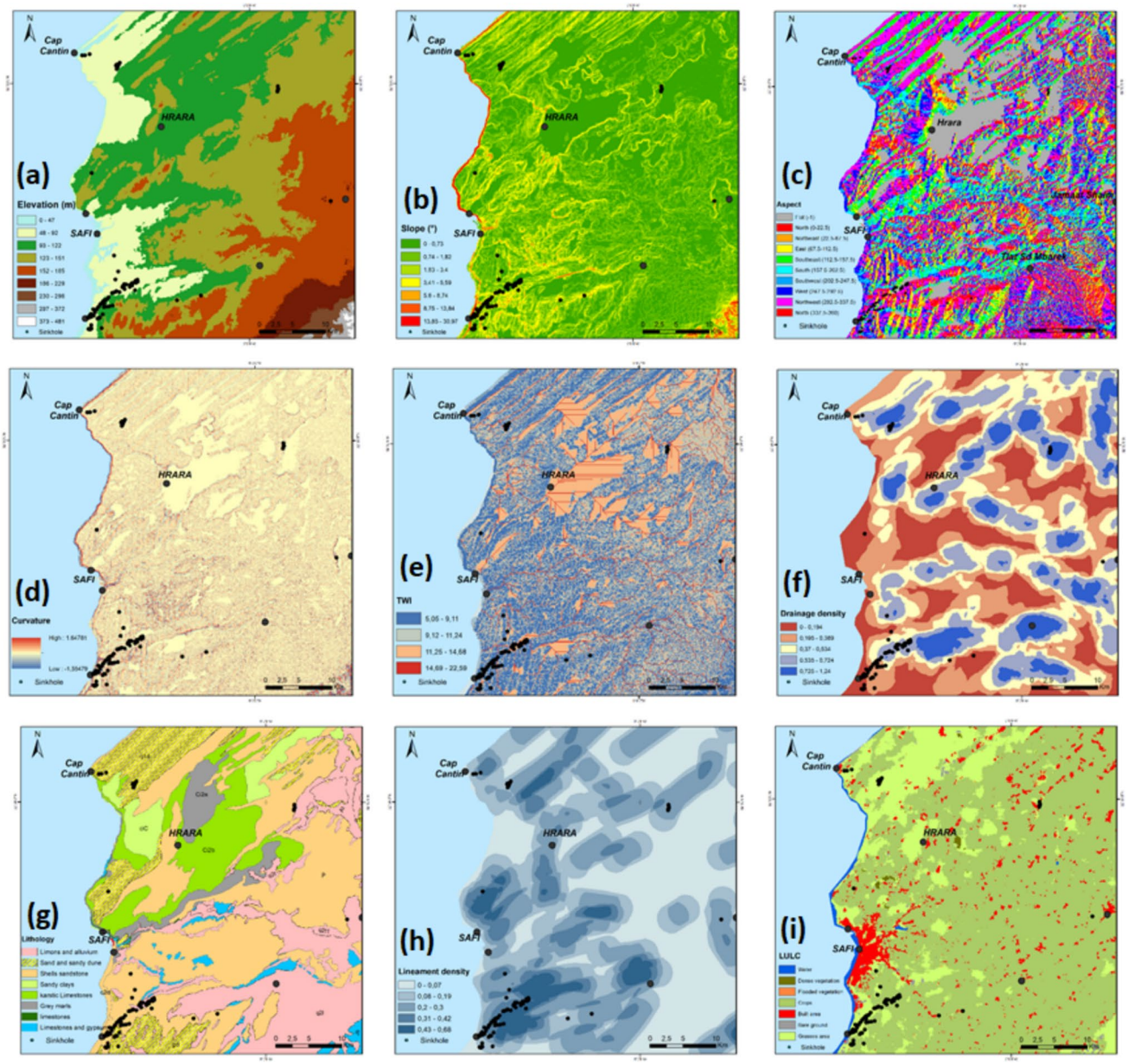

Fig. 6 Conditioning factors for sinkhole susceptibility mapping: (**a**) Elevation, (**b**) Slope, (**c**) Aspect, (**d**) Curvature, (**e**) TWI, (**f**) Drainage density, (**g**) Lithology, (**h**) Lineament density and (**i**) Land Cover/Use. (Spatial resolution for all condition factors is 30 m × 30 m)

Both the Frequency Ratio and Analytical Hierarchy Process methods offer valuable insights into sinkhole susceptibility mapping. The FR method is relatively straightforward and data-driven, while the AHP method allows for the integration of expert knowledge and a more systematic consideration of criteria importance. Validation is crucial for assessing the reliability of both models and ensuring their applicability to real-world conditions.

Results

The characterization of sinkholes through morphometric analysis, specifically the elongation ratio (Er), offers valuable insights into their shapes and dimensions (Gutiérrez, 2005). Sinkholes can be classified into distinct shapes based on their Er values, ranging from circular to elongated (Basso et al. 2013; Kobal et al. 2015). In our study, the

morphometric analysis revealed a diverse array of sinkhole shapes. Approximately 45.16% of the sinkholes exhibited a circular form, emphasizing a balanced relationship between length and width. A notable 16.13% were categorized as sub-circular, indicating a slightly more elongated configuration. Further diversity emerged with 22.58% displaying an elliptical shape, 13% identified as sub-elliptical, and a distinct 3.23% characterized as elongated (Fig. 6). The prevalence of circular sinkholes, with a maximum diameter of 80 m, suggests the relative youthfulness of these karst systems (Brinkmann et al. 2008; Kobal et al. 2015). Additionally, the maximum depths observed for each shape category contribute to a comprehensive understanding of the varied morphologies within the study area, with circular sinkholes reaching depths of 23.8 m, elliptical sinkholes descending to 40.4 m, and elongated sinkholes reaching depths of 25 m (Fig. 7). This detailed morphometric analysis enhances our appreciation of the geological diversity and evolution of sinkholes in the examined region.

Analytic Hierarchy Process (AHP)

The Analytic Hierarchy Process (AHP) stands out as a structured and hierarchical decision-making methodology that seamlessly incorporates both quantitative and qualitative analyses. As elucidated by Wang and Li (2017), AHP serves as a powerful tool that amalgamates data, knowledge, and subjective judgments of analysts to evaluate the susceptibility of sinkhole collapse. In the context of this study, a weighted linear combination method is deployed to predict sinkhole susceptibility, encompassing a comprehensive consideration of nine carefully selected controlling factors, each with its corresponding classes or sub-criteria (Fig. 8).

To verify the significance of each factor in the context of sinkhole occurrence, initial paired comparisons are conducted on square matrices, assigning weights to both criteria and sub-criteria. The determination of the relative importance of each factor is achieved through Saaty's (1980) ranking scale for pairwise comparisons, where values between 1 and 9 signify the relative dominance of one factor over another in the context of sinkhole formation (refer to Table 2).

The consistency ratio (CR) can be used in AHP to determine the matrix's consistency (Tzeng and Huang 2011). Equation (1) is used to calculate the consistency ratio, which is a metric of the judgement about a decision made at random (Tzeng and Huang 2011)

$$\mathrm{CR} = \frac{\mathrm{CI}}{\mathrm{RI}} \tag{1}$$

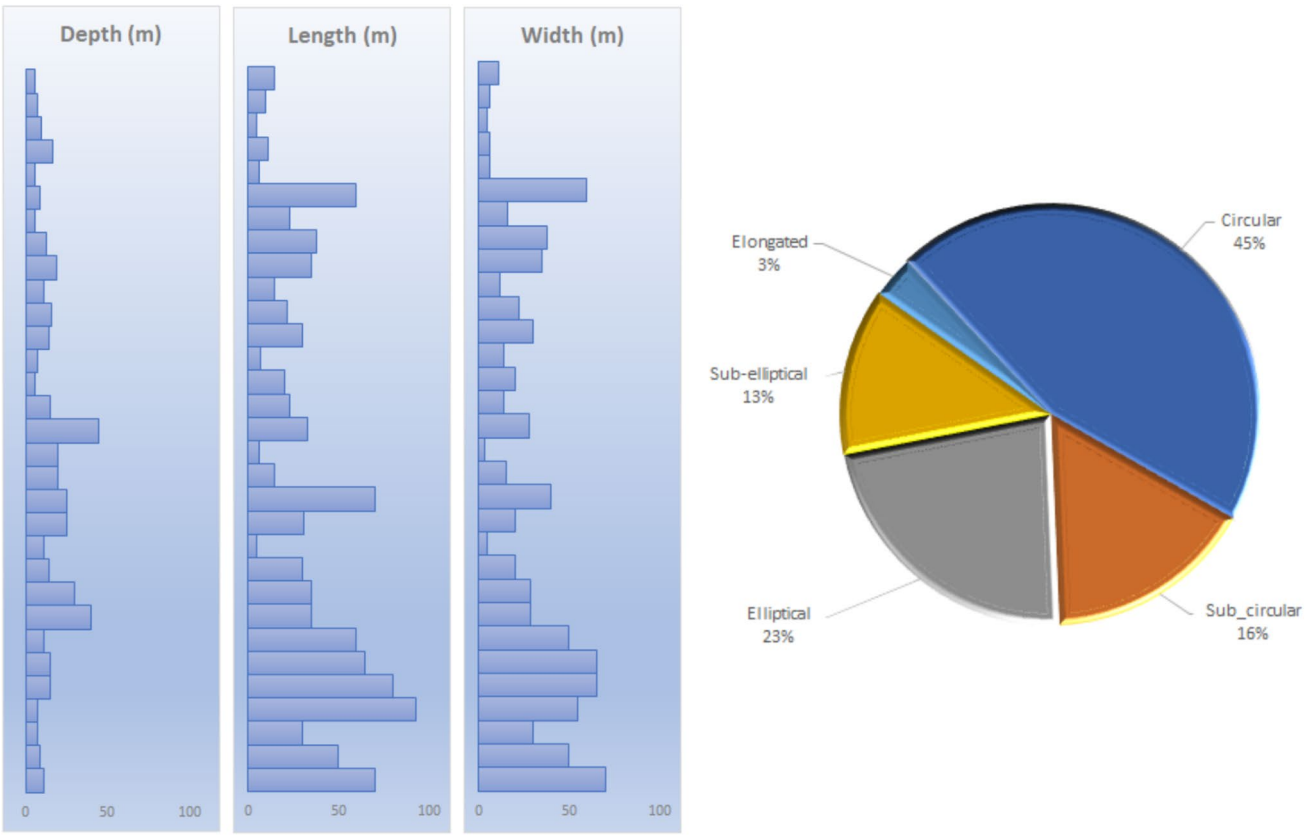

Fig. 7 Sinkhole size (depth, length and width) and shape distribution

	Elevation	Slope	Aspect	Curvature	TWI	Lithology	LULC	LD	DD	Weights
Elevation	1									0,0265604
Slope	2	1								0,0506779
Aspect	2	1/2	1							0,0359293
Curvature	5	2	3	1						0,08802
TWI	3	3	4	1/2	1					0,0841008
Lithology	7	5	6	5	3	1				0,2312181
LULC	3	2	3	3	2	1/3	1			0,1023991
LD	6	3	4	3	3	2	3	1		0,2320534
DD	5	3	4	2	2	1/2	3	1/2	1	0,149041

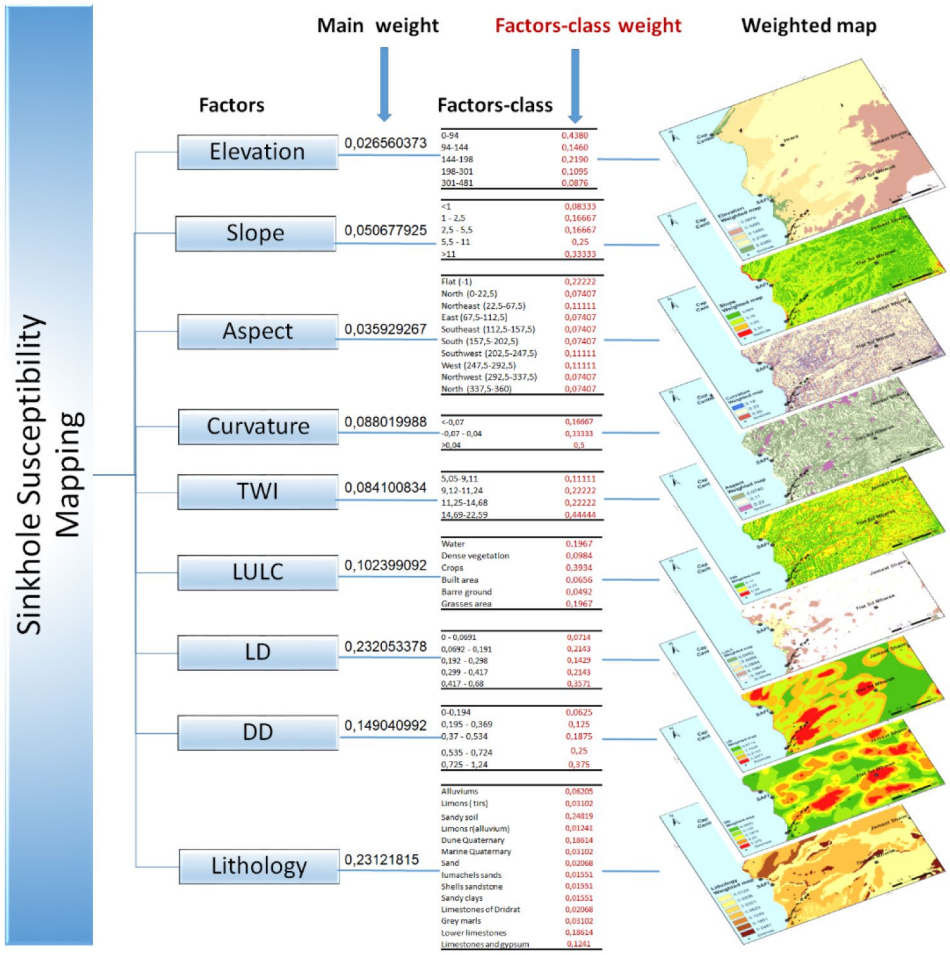

Fig. 8 Sinkhole susceptibility inducing factors and factors classes weights

Table 2 Basic ranking model for pairwise comparison (Saaty 1980)

Description	Value
Equal importance	1
Moderate importance of one over another	3
Strong importance	5
Very strong	7
Extremely high importance	9
Intermediate values	2,4,6,8

where CI is the Consistency Index defined by the Eq. (2):

$$CI = \frac{\lambda max - n}{n - 1} \quad (2)$$

where "λmax is the largest eigenvalue of a preference matrix and n is the number of parameters" (Ying et al., 2007; Thanh and De Smedt, 2012, Taheri et al., 2019).

RI is the random consistency index, established by Saaty (1990) as a function of n (see Table 3).

For a value of Consistency ratios more than 0.1, it's suggest that the comparisons and scores should be modified. In this study we have selected nine factors. Consequently, RI is 1.45 according to Saaty (1977), and CR is 0.051 according to Eq. (1). The calculated consistency ratio is lower than 0.1, indicating paired comparisons were coherent. In this study, the sinkhole susceptibility index has been generated through a weighted linear combination (WLC) of the influencing factors and the classes of each factor (Voogd 1983). The Sinkhole susceptibility index (SSI) is calculated by adding the products of the weights allocated to each factors and classes of factors, following to equation:

$$\mathrm{SSI} = \sum_{i=1}^{n} W_i * w_{ji} \quad (3)$$

where Wi denotes the weights assigned to each conditioning component (i) wji is the weight assigned to class j of factor I and n denotes the total number of factors taken into account in the model. Based on natural breaks method, the resultant SSI-map was divided into five classes (very low, low, moderate, high, and very high).(Fig. 9).

Frequency Ratio (FR)

The Frequency Ratio (FR) model, a bivariate statistical approach, is employed in this study to assess the influence of controlling factors on sinkhole occurrence, as established by Lee and Pradhan (2007). This model establishes a spatial relationship between the sinkhole inventory and these factors, allowing for a thorough examination of their impact (Demir et al. 2014; Park et al. 2012; Lee and Pradhan 2007).

Table 3 Assigning of RI (Saaty 1977)

Nnumber of factors	1	2	3	4	5	6	7	8	9	10
RI	0.00	0.00	0.58	0.90	1.12	1.24	1.32	1.41	1.45	1.49

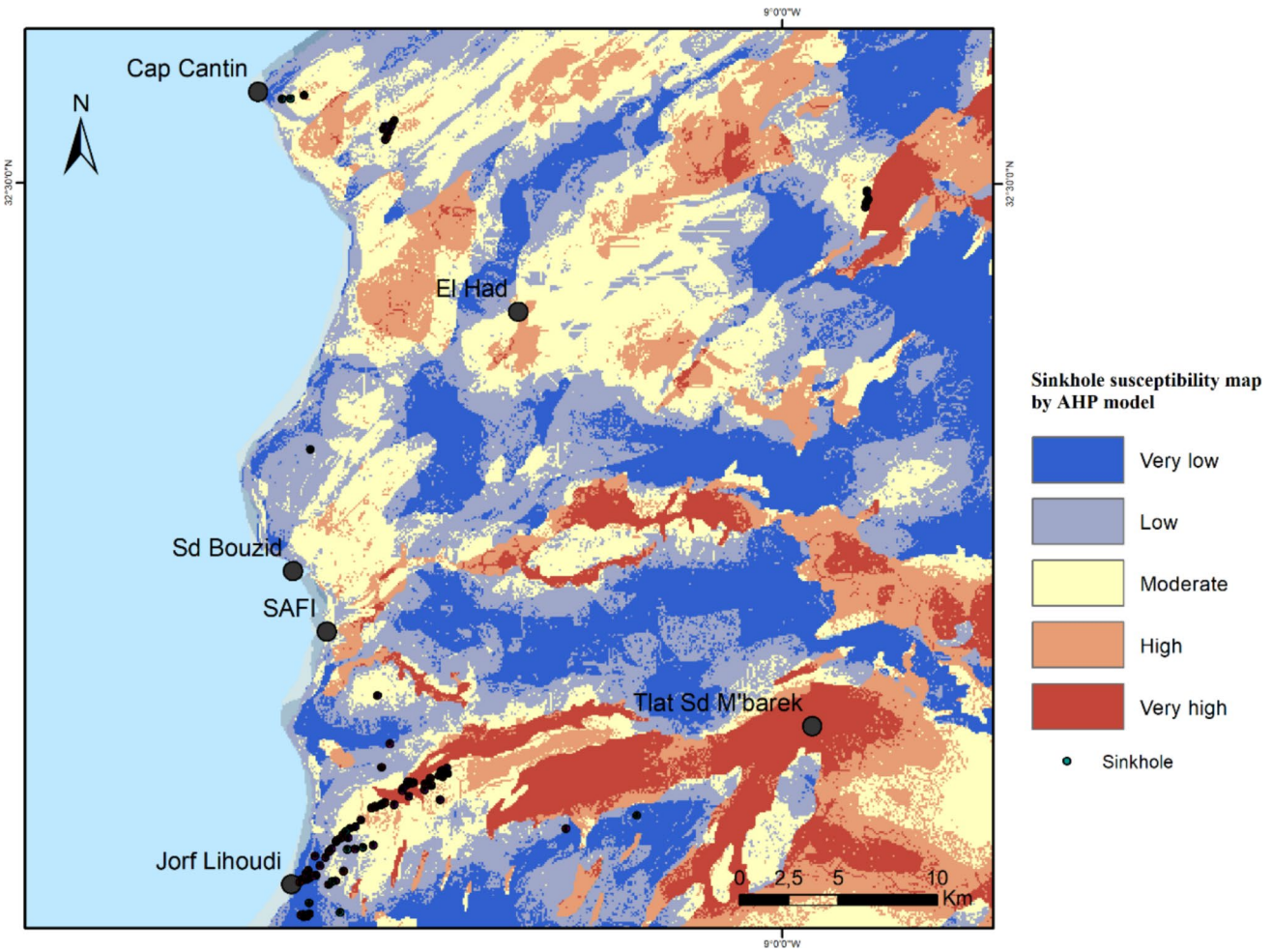

Fig. 9 Sinkhole susceptibility map by using AHP model

The frequency ratio, a key metric in this model, denotes the ratio of the percentage of areas where sinkhole collapse has occurred in a specific class to the percentage area of the impacting class relative to the entire study area.

In this analysis, the FR model is applied to evaluate sinkhole susceptibility, considering nine factors (see Fig. 6), and utilizing 104 sinkhole locations, segregated into training (70%) and validation (30%) datasets (see Fig. 10). The sinkhole susceptibility map is generated through the weighted overlay function in a GIS environment, enabling the amalgamation of various factors and their allocation to the ratio (Oh et al. 2011).

The resulting sinkhole susceptibility values are categorized into five classes: very high, high, moderate, low, and very low, using the natural break method, a classification approach commonly employed in landslide susceptibility mapping (Falaschi et al. 2009; Bednarik et al. 2010; Pourghasemi et al. 2012, 2013). This systematic approach provides a comprehensive understanding of the spatial distribution and susceptibility levels of sinkholes in the study area.

The Frequency Ratio (FR) model has demonstrated extensive and effective applicability in the realm of landslide susceptibility mapping, as illustrated by numerous studies (e.g.,

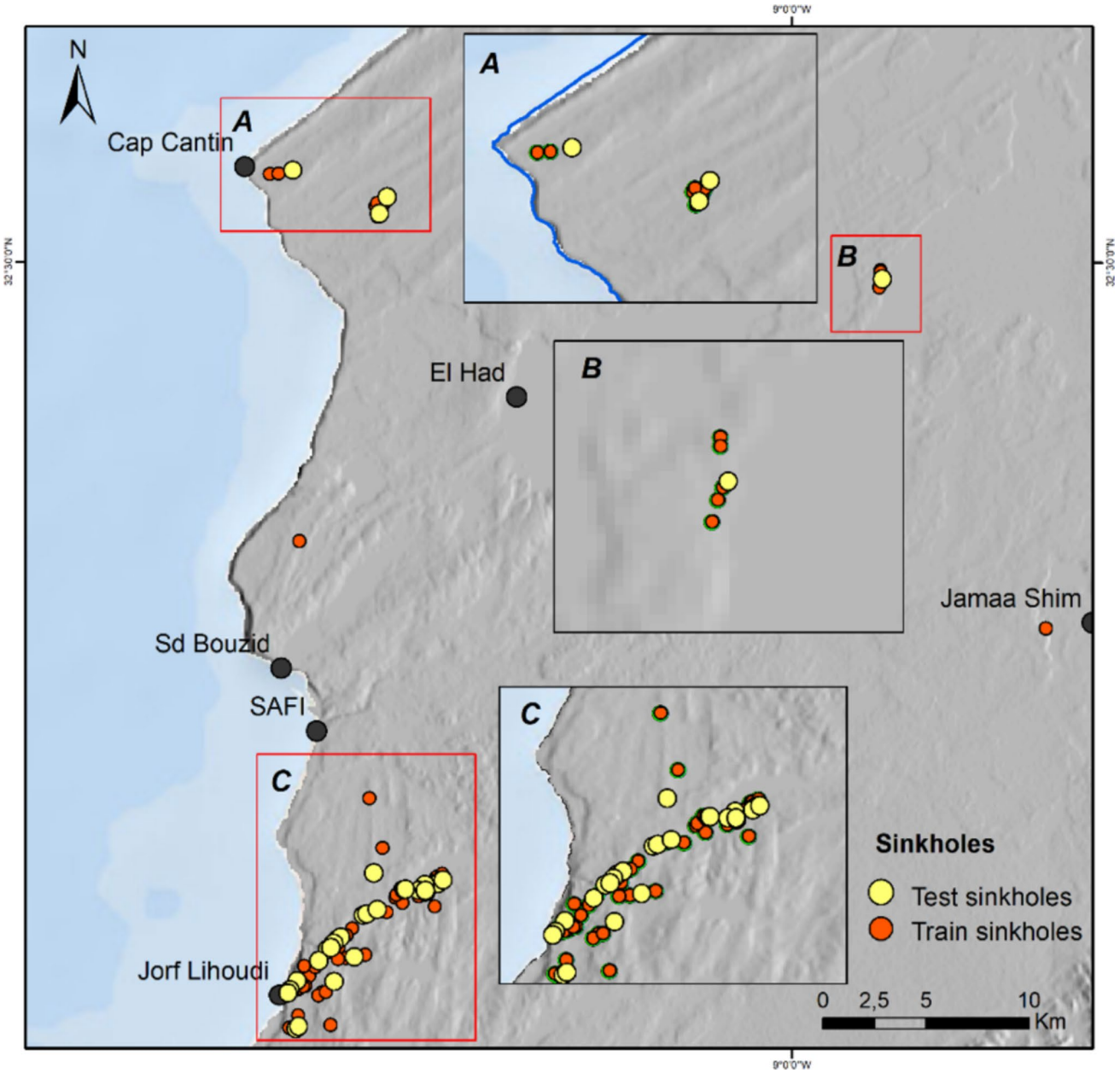

Fig. 10 Testing and training sinkhole location

Yilmaz 2009; Umar et al. 2014; Wu and Wu 2016; Wang et al. 2016, Wang and Li 2017). This model relies on establishing correlations between the sinkhole inventory and the factors that contribute to sinkhole collapse (Reis et al. 2012). By combining the sinkhole inventory map with factor maps, the frequency ratio (FR) for each class of causal factors is derived using Eq. (4) (Mondal and Maiti 2013). This approach allows for a quantitative assessment of the influence of various factors on sinkhole susceptibility, providing valuable insights for the mapping process in the coastal area of Safi.

$$\mathrm{FR} = \frac{N_i^p / N}{N_i^{lp} / N^l} \tag{4}$$

where N_i^p is the number of pixels in each sinkhole conditioning factor class, N is the total number of pixels in the all study area. N_i^{lp} is the number of sinkhole collapse pixels in each sinkhole conditioners factor class, N^l is the total number of Sinkhole collapse pixels in the entire study area (Table 4).

The calculated frequency ratio is added to generate a Sinkhole Susceptibility Index (SSI) map by using Eq. (5) (Lee and Talib 2005)

$$SSI = \sum_{i=1}^{n} FR_i \tag{5}$$

where Fr is the frequency ratio, and n is the number of relevant causal factors. The model calculates the ratio of the area where sinkhole collapses occurred to the total area, with a value of "1" indicating an average correlation, values greater than "1" signifying a high correlation, and values less than "1" indicating a low correlation between collapses and factor classes (Akgun et al. 2007). Results obtained from applying the Frequency Ratio (FR) model, as shown in Table 4, facilitated the establishment of correlation patterns between sinkhole collapse occurrences and classes of causal factors. Concerning lithology, areas featuring upper Jurassic limestone and gypsum, limestone from the Dridrat formation, and consolidated dune of Plioquaternary exhibited FR values greater than 1, suggesting a higher likelihood of sinkhole collapse.

In terms of slope, areas with slopes of less than 10 degrees and altitudes under 100 m, along with slope aspects facing north, south, and southeast, demonstrated FR values greater than 1, indicating a higher potential for collapse occurrence.

Regarding curvature, the flat surface class had the highest FR value (1.20), followed by the concave class (1.08), and then the convex class (0.93).

For lineament density, areas with a density greater than 0.3 showed a high possibility of collapse occurrence, with an FR value of 5.4. Conversely, areas with a density less than 0.3 had an FR ratio of less than 1, indicating a lower probability of collapse occurrence.

Concerning drainage density, areas with a density ranging from 0.53 to 0.72 and greater than 0.73 exhibited FR values of 2.23 and 1.32, respectively, suggesting varying degrees of susceptibility to collapse.

Lastly, in the case of land use, areas classified as "gasses" showed an FR value of 2.27, indicating the highest possibility of collapse incidence.

In the GIS environment, the overlay technique was employed to combine the nine factors allocated to the ratio, thereby establishing the Frequency Ratio (FR) of sinkhole susceptibility. The resulting sinkhole susceptibility index map was reclassified to create a sinkhole collapse susceptibility map, which is categorized into five classes using the natural breaks method: very low, low, moderate, high, and very high (Fig. 11).

Results and discussion

The results of the sinkhole susceptibility mapping using both the Frequency Ratio (FR) and Analytical Hierarchy Process (AHP) models offer valuable insights into the spatial distribution and potential risk zones of sinkhole occurrences in the coastal area of Safi, Morocco.

Sinkhole collapse is prevalent in specific regions of the study area, particularly in the southern part of Safi (Jorf Lihoudi region) and the northeastern region in Moul Bergui, following the N-S to NE-SW lineament direction (Fig. 10B,C). These sinkholes exhibit circular shapes and vary in diameter from 10 to 400 m, with smaller sinkholes, ranging from 15 to 50 m in diameter, having depths up to 40 m. The localization of sinkholes is closely tied to controlling factors such as lithology, notably Upper Jurassic evaporitic-limestone, and Plio-Quaternary biodetritic limestone. The presence of evaporitic limestone outcrops in the southern region is a key factor contributing to the numerous sinkholes observed.

The rapid development of karst forms in the region is elucidated by Weisrock and Lunski (1987), attributing it to the presence of underlying gypsum and anhydrite, intense fracturing, and past humid paleo-climates. Eustatic variations in the marine base level, favoring the sinking of the hydrographic network during regressions, are also highlighted. The distribution of collapse sinkholes in a NE-SW direction appears to be influenced by these tectonic structures. Moreover, topographic factors such as slope, curvature, elevation, land use, and drainage systems play crucial roles.

The sinkhole susceptibility mapping, employing both the Analytical Hierarchy Process (AHP) and Frequency Ratio

Table 4 Sinkhole collapse conditioning factors and its Frequency Ratio values

Factor	Class-Factor	% class_pixel	class_area	%CS_pixel	FR
lineament density	0–0,0691	42,84	899,81	1,39	0,03
	0,0692—0,191	20,24	12,597,29	19,44	0,96
	0,192 −0,298	26,62	17,096,33	26.39	0,95
	0,299—0,417	6,92	24,294,78	37,50	5,42
	0,417 −0,68	3,37	9897,87	15,28	4.5
Drainage density					
	0–0,194	9,57	4499,03	6,94	0,73
	0,195—0,369	27,54	13,497,10	20,83	0,76
	0,37—0,534	27,13	4499,03	6.94	0,26
	0,535–0,724	19,93	28,793,81	44,44	2.23
	0,725- 1,24	15,84	13,497,10	20,83	1,32
LULC					
	Water	0,03	0,00	0,00	0,00
	Dense vegetation	0,25	0,00	0,00	0,00
	Crops	75,36	35,092,46	54,17	0.7
	Built area	5.18	1799,61	2,78	0.54
	Barre ground	0,20	0,00	0,00	0,00
	Grasses area	18,98	27,894,01	43,06	2,2
Aspect					
	Flat (−1)	10,83	10,797,68	16,67	1,54
	North (0–22,5)	6,75	7198,45	11,11	1,65
	Northeast (22,5–67,5)	7,76	1799,61	2,78	0,36
	East (67,5–112,5)	7,41	4499,03	6,94	0,94
	Southeast (112,5–157,5)	10,45	10,797,68	16,67	1,59
	South (157,5–202,5)	8,09	7198,45	11,11	1,37
	Southwest (202,5–247,5)	8,41	2699,42	4,17	0.50
	West (247,5–292,5)	13,25	5398,84	8,33	0,63
	Northwest (292,5–337,5)	20,54	11,697,49	18.06	0,85
	North (337,5–360)	6,51	2699,42	4,17	0,64
Elevation					
	0–94	0,94	1799,61	2,78	2,95
	94–144	10,96	47,689,76	73,61	6,72
	144–198	42.57	13,497,10	20.83	0,49
	198–301	31.26	1799,61	2,78	0.09
	301–481	14,27	0,00	0,00	0,00
Slope					
	0–0,971	59,34	25,194,59	38.89	0,66
	0,971–2,55	27,42	29,693,62	45,83	1.67
	2,550–5,465	10,37	8998,07	13,89	1,34
	5,465–10,808	2,38	899,81	1,39	0,58
	10,808–30,966	0,49	0,00	0,00	0,00
Curvature					
	<—0,07	15,41	10,797,68	16,67	1,08
	−0,07 −0,04	16,24	12,597,29	19,44	1,20
	>0,04	68,35	41,391,11	63,89	0,93
TWI					
	5,05–9,11	38,34	31,493,23	48,61	1,27
	9,12–11,24	34,78	13,497,10	20,83	0,60
	11,25–14,68	21.98	14,396,91	22,22	1,01
	14,69–22,59	4,90	5398,84	8,33	1,70
Lithology					
	Alluviums	0.10	0,00	0,00	0,00
	Limons (tirs)	1,24	0,00	0,00	0,00
	Sandy soil	7.86	0,00	0,00	0,00
	Limons r[alluvium)	2,50	0,00	0,00	0,00

Table 4 (continued)

Factor	Class-Factor	% class_pixel	class_area	%CS_pixel	FR
	Dune Quaternary	6,07	11,059,30	7,70	1,27
	Marine Quaternary	0,25	0,00	0,00	0,00
	Sand	0,04	0,00	0,00	0,00
	lumachels sands	2,73	0,00	0,00	0,00
	Shells sandstone	9,86	0,00	0,00	0,00
	Sandy clays	25,40	8998,07	10,89	0,43
	Limestones of Dridrat	13,70	13,497,10	20,83	1,52
	Grey marls	2,96	899,81	1,39	0,47
	Lower limestones	0,33	0,00	0,00	0,00
	Limestones and gypsum	26,96	30,331,81	59.19	2,20

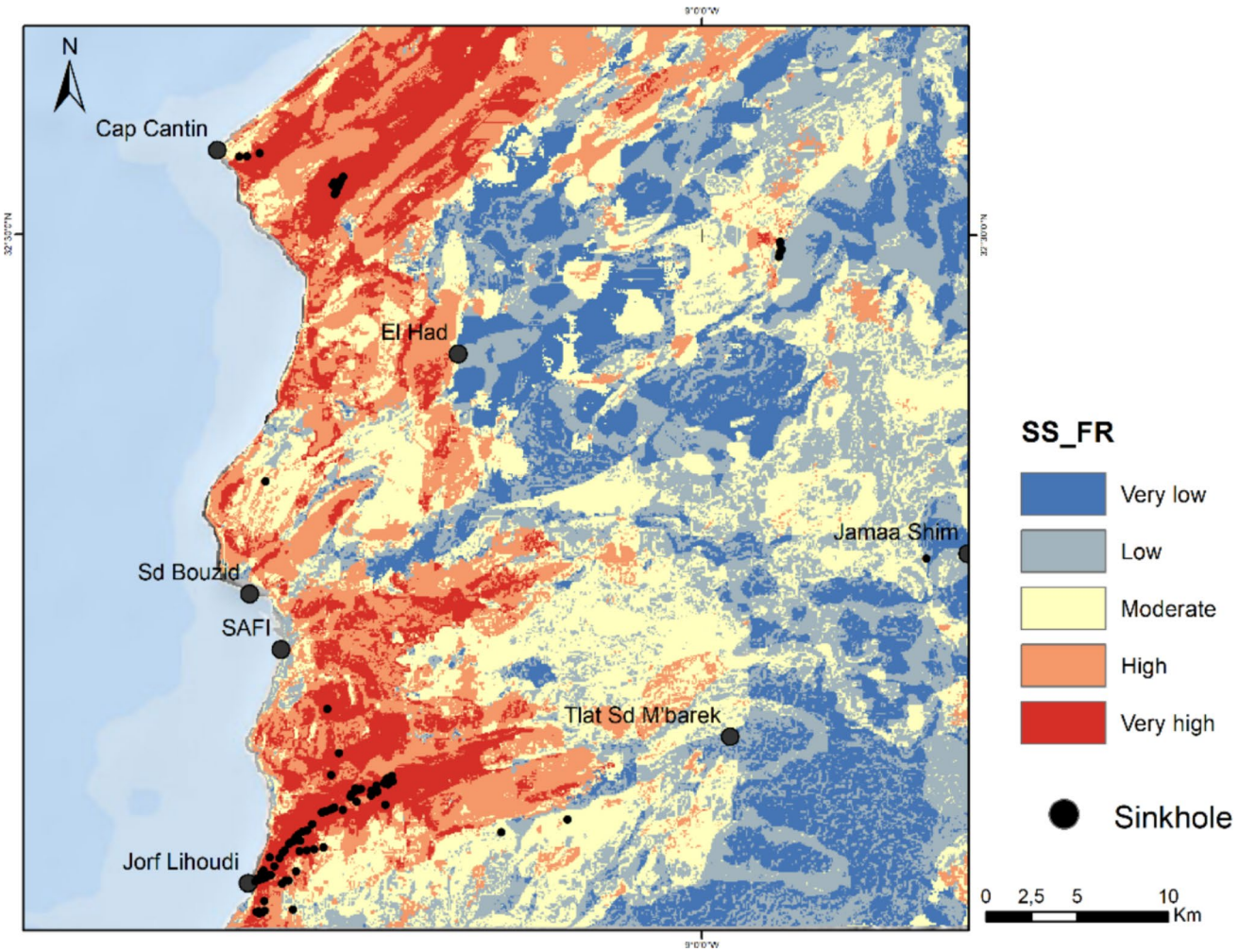

Fig. 11 Sinkhole susceptibility map using Frequency Ratio (FR) model

(FR) methodologies, reveals a significant spatial dominance of high and very high susceptibility levels in Safi's southern and northeastern regions. These vulnerabilities are linked to lithological factors, including limestones, gypsum, and sandstone, as well as the influence of NE-SW lineaments and topographic features. The comprehensive analysis provides crucial insights for understanding the distribution and influencing factors of sinkhole susceptibility, offering practical implications for land use planning, infrastructure development, and hazard mitigation in the coastal region of Safi. The chosen approach emphasizes a rigorous validation process, using the Area Under Curve (AUC) method to ensure the reliability and accuracy of the susceptibility maps by comparing them to observed sinkhole occurrences.

The integration of both FR and AHP methods enhances the validation's comprehensiveness, aiming to provide a robust and trustworthy sinkhole susceptibility map that can confidently guide decision-making and future research endeavors in the area. Validation using the AUC technique shows that the AHP and FR models achieve success rates of 73.5% and 90.5%, respectively (Fig. 12). The outcomes demonstrate that both models are capable of making accurate predictions, further supporting their utility in assessing and managing sinkhole risks in the Safi coastal region.

The models were evaluated by comparing the susceptibility maps with the known locations of sinkholes. Both the AHP and FR analyses resulted in susceptibility maps that were overlaid with all 104 sinkhole locations. The stacking process of the FR-based sinkhole susceptibility map with the total, training, and testing sinkholes showed that 78.85%, 76.71%, and 83.87% of the identified sinkholes, respectively, were concentrated in the high to very high susceptibility class.

The sinkhole susceptibility map generated using the FR approach revealed that low susceptibility zones accounted for 44.3% of the total area. Moderate, high, and very high sinkhole susceptibility zones represented 32%, 16.1%, and 7.6% of the entire area, respectively.

Conclusion

The sinkhole susceptibility analysis involves the integration of diverse datasets, including digital elevation models, geological maps, satellite images, and field data. The mapping process considers nine influencing factors, and sophisticated modeling techniques are applied to produce accurate susceptibility maps. The chosen AHP and FR methods offer a balanced approach, with AHP incorporating expert judgment and pairwise comparisons and FR providing simplicity and computational efficiency.

The results of the study reveal that the southern and northeastern regions of the study area are spatially dominated by high and very high susceptibility levels. This vulnerability is attributed to lithological aspects, tectonic structures, and topographic factors. The sinkhole inventory compiled through extensive fieldwork enhances the accuracy of the susceptibility mapping, and the validation process demonstrates the reliability of the applied methodologies.

The morphometric analysis of sinkholes highlights their diverse shapes and dimensions, providing insights into their geological diversity and evolution. The study emphasizes the significance of both AHP and FR methods in providing a comprehensive understanding of sinkhole susceptibility, with the FR model demonstrating higher accuracy in the validation process.

In conclusion, the sinkhole susceptibility mapping in the coastal area of Safi contributes valuable insights for hazard mitigation, land use planning, and risk management. The findings of this study provide a foundation for future research in geohazard assessment and serve as a practical resource for decision-makers involved in the development and environmental management of regions susceptible to sinkhole collapses. The integration of fieldwork, remote sensing, and various spatial data sources ensures a robust foundation for sinkhole susceptibility mapping, enhancing accuracy and reliability in geoscientific research.

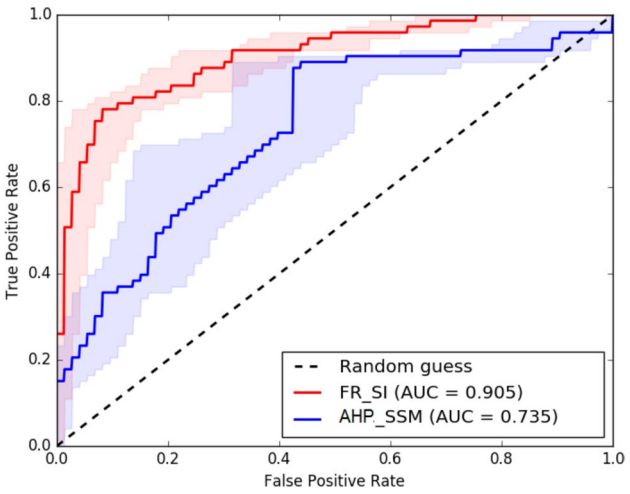

Fig. 12 ROC curves for the sinkhole susceptibility maps

References

Akgun A, Dag S, Bulut F, Durmaz S (2007) Landslide susceptibility mapping for a landslide-prone area (Findikli, NE of Turkey) by likelihood-frequency ratio and weighted linear combination models. Environ Geol 53(8):1477–1486

Aurit MD, Paterson RO, Blanford JI (2013) A GIS analysis of the relationship between sinkholes, dry-well complaints and groundwater pumping for frost-freeze protection of winter strawberry production in Florida. PLoS ONE 8:1–9

Basso A, Bruno E, Parise M, Pepe M (2013) 2013) Morphometric analysis of sinkholes in a karst coastal area of southern Apulia (Italy. Environ Earth Sci 70:2545–2559. https://doi.org/10.1007/s12665-013-2297-z

Bednarik M, Magulova B, Matys M, Marschalko M (2010) Landslide susceptibility assessment of the Kralovany-Liptovsky Mikulas railway case study. Phys Chem Earth 35:162–171

Brinkmann R, Parise M, Dye D (2008) Sinkhole distribution in a rapidly developing urban environment: Hillsborough County, Tampa Bay area, Florida. Eng Geol 99:169–184

Ciotoli G, Di Loreto E, Finoia M, Liperi L, Meloni F, Nisio S, Sericola A (2016) Sinkhole susceptibility, Lazio Region, central Italy. J Maps 12:287–294. https://doi.org/10.1080/17445647.2015.1014939

Constantin A, Tămas T, Kacsoh D (2011) Environmental problems in karst areas. Environ Eng Manag J 10(11):1639–1645

Demir T, Aytek A, Gokceoglu C (2014) A new approach to estimate slope instability: the case of quarry slopes in the carbonate rocks of the Antalya complex, SW Turkey. Environ Earth Sci 72(6):1993–2008

Dai J, Lei M, Liu W, Tang S, Lai S (2008) An assessment of karst collapse hazards in Guilin, Guangxi Province, China. In:Yuhr LB., Alexander CE Jr, Beck BF, (eds.) Sinkholes and the engineering and environmental impacts of karst (Geotechnical Special Publication No. 183) ASCE, pp 156–164

Dogan U, Yilmaz M (2011) Natural and induced sinkholes of the Obruk Plateau andKarapinar–Hotamis Plain, Turkey. J Asian Earth Sci 40:496–508

Falaschi F, Giacomelli F, Federici PR, Puccinelli A, D'Amato AG, Pochini A, Ribolini A (2009) Logistic regression versus artificial neural networks: landslide susceptibility evaluation in a sample area of the Serchio River valley, Italy. Nat Hazards 50:551–569

Ferré M, et Ruhard JP (1975) Ressources en eau t2 (plaines et bassins du Maroc Atlantique); les bassins des Abda-Doukkala et du Sahel d'Azemmour à Safi. Notes mém. Serv. géol. Maroc, n°231

Ford DC, Williams P (2007) Karst hydrogeology and geomorphology. John Wiley, Chichester, p 562. https://doi.org/10.1002/9781118684986

Galve JP, Remondo J, Gutiérrez F, Lucha P, Bonachea J (2009) Morphometric and morphogenesis characterization of sinkholes developed on evaporite rocks. Geomorphology 105(1–2):154–164

Gao Y, Alexander EC (2003) Spatial analysis of sinkhole density using GIS and kernel density estimation. Environ Eng Geosci 9(2):135–143

Gigout M (1951) Etudes geologiques sur la Méseéta marocaine occidentale (Arriére-pays de Casablanca, Mazagan et Safi). Imprimerie Maroc-Matin, p 507.

Gigout M (1954) Carte géologique de la Méséta entre Mechrâ Benâbbou et Safi (Abda. Service géologique du Maroc, Institut géographique national, Maroc, Doukkala et Massif des Rehamna)

Goudie A (2013) Encyclopedia of geomorphology. Routledge

Gutiérrez F, Calaforra JM, Cardona F, Ortı F, Duran JJ, Garay P (2008a) Geological and environmental implications of evaporite karst in Spain. Env Geol 53:951–965

Gutiérrez F, Parise M, De Waele J, Jourde H (2014) A review on natural and human-induced geohazards and impacts in karst. Earth Sci Rev 138:61–88. https://doi.org/10.1016/j.earscirev.2014.08.002

Gutiérrez F, Cooper AH, Johnson KS (2008b) Identification, prediction and mitigation of sinkhole hazards in evaporite karst areas. Env Geol 53:1007–1022

Gutiérrez F, Guerrero J, Lucha P (2008c) A genetic classification of sinkholes illustrated from the Ebro valley evaporite alluvial karst (NE Spain). Env Geol 53:993–1006

Gutiérrez F, Guerrero J, Lucha P (2008d) Quantitative sinkhole hazard assessment: a case study from the Ebro valley evaporite karst (NE Spain). Nat Hazards 45:211–233

Gutiérrez F, Galve JP, Guerrero J, Lucha P, Cendrero A, Remondo J, Bonachea J, Gutierrez M, Sanchez JA (2007) The origin, typology, spatial distribution and detrimental effects of the sinkholes developed in the alluvial evaporite karst of the Ebro River valley downstream of Zaragoza city (NE Spain). Earth Surf Process Landforms 32(6):912–928

Gutiérrez F, Galve JP, Lucha P, Bonachea J, Jorda´ L, Jorda R (2009) Investigation of a large collapse sinkhole affecting a multi-storey building by means of geophysics and the trenching technique (Zaragoza city, NE Spain). Environ Geol 58:1107–1122. https://doi.org/10.1007/s00254-008-1590-8

Gutiérrez F, Cardona F, Calaforra JM, Durán JJ, Garay P (2005) Geological and environmental implications of evaporite karst in Spain. Abstracts of the 6th International Conference on Geomorphology, Zaragoza (Spain)

Guzzetti F, Carrara A, Cardinali M, Reichenbach P (1999) Landslide hazard evaluation: a review of current techniques and their application in a multi–scale study, Central Italy. Geomorphology 31:181–216. https://doi.org/10.1016/S0169-555X(99)00078-1

Kaufmann G (2014) Geophysical mapping of solution and collapse sinkholes. J Appl Geophys 111:271–288

Khouz A, Trindade J, Oliveira S, El Bchari F, Bougadir B, Ricardo GR, Jadoud M (2022) Landslide susceptibility assessment in rocky coast subsystem of Essaouira coastal area – Morocco. Nat Hazards Earth Syst Sci 22:3793–3814. https://doi.org/10.5194/nhess-22-3793-2022

Kobal M, Bertoncelj I, Pirotti F, Dakskobler I, Kutnar L (2015) Using lidar data to analyse sinkhole characteristics relevant for understory vegetation under forest cover—case study of a high karst area in the Dinaric Mountains. PLoS ONE. https://doi.org/10.1371/journal.pone.0122070

Komac MA (2006) Landslide susceptibility model using the analytical hierarchy process method and multivariate statistics in perialpine Slovenia. Geomorphology 74:17–28

Laaziz YA, Souhel A, Laylman M, Elaabasi M, El Bchari F (2016) Geospatial modeling for karstic collapse probability map in the Doukkala basin (Morocco). Arab J Geosci 3(2):6–16

Lamelas MT, Marinoni O, Hoppe A, De La Riva J (2008) Doline probability map using logistic regression and GIS technology in the central Ebro Basin (Spain). Environ Geol 54(5):963–977

Lee S, Pradhan B (2007) Landslide hazard mapping at Selangor, Malaysia using frequency ratio and logistic regression models. Landslides 4(1):33–41

Lee S, Talib JA (2005) Probabilistic landslide susceptibility and factor effect analysis. Environ Geol 47(7):982–990

Michard A (1976) Contribution à l'étude des karsts du Maroc atlantique. Travaux De L'institut Scientifique Chérifien, Série Géologie Et Géographie Physique 27:1–79

Mondal M, Maiti R (2013) Landslide susceptibility analysis in Darjeeling Himalayas of India: a GIS-based statistical approach. Nat Hazards 65(1):443–460

Oh H, Kim J-K, Lee S (2011) Gis mapping of regional probabilistic groundwater potential in the area of Pohang city, Korea. J Hydrol 399:158–172

Ouadia M, Aberkan M, Boualla O (2008) The karstificationmarvels and the risks in the Plioquaternary formations of the inshore zone of the Doukkala-Abda (Morocco) Actes RQM4. Oujda 2008:40–48

Ozdemir A (2015) Sinkhole susceptibility mapping using a frequency ratio method and GIS technology near Karapinar, Konya Turky. Procedia Earth Planet Sci 15(2015):502–506. https://doi.org/10.1016/j.proeps.2015.08.059

Paine JG, Buckley SM, Collins EW, Wilson CR (2012) Assessing collapse risk in evaporite sinkhole-prone areas using microgravimetry and radar interferometry. Jeeg 17:75–87. https://doi.org/10.2113/JEEG17.2.75

Parise M (2010) Hazards in karst, in Sustainability of the Karst Eenvironment: Dinaric Karst and Other Karst Regions, Bonacci, O., ed., IHP-VII UNESCO, Series on Groundwater. 2:155−162.

Park S, Choi C, Kim B, Kim J (2012) Landslide susceptibility mapping using frequency ratio, analytic hierarchy process, logistic regression, and artificial neural network methods at the Inje area. Korea Environ Earth Sci 68:1443–1464

Pourghasemi HR, Pradhan B, Gokceoglu C (2012) Application of fuzzy logic and analytical hierarchy process (AHP) to landslide susceptibility mapping at Haraz watershed, Iran. Nat Hazards 63:965–996

Pourghasemi HR, Moradi HR, Fatemi Aghda SM (2013) Landslide susceptibility mapping by binary logistic regression, analytical hierarchy process, and statistical index models and assessment of their performances. Nat Hazards 69:749–779

Praveen A, Janardhana MR, Gowtham S, Sajinkumar KS (2019) Delineation of sinkhole-prone areas using frequency ratio, analytic hierarchy process, and geographical information system techniques. Environ Earth Sci 78(2):67

Reis F, Oliveira R, Ribeiro A, Lobo A (2012) Landslide susceptibility analysis using GIS and multivariate statistical analysis: a case study from the area north of Lisbon (Portugal). Nat Hazards 61(1):421–435

Renault P (1970) Le karst du Jebel Ouarkziz (Sahara Atlantique). Spéléo-Club De Paris, Bulletin 70:209–216

Roch A (1950) Contribution à l'étude géomorphologique des karsts marocains. Travaux De L'institut Scientifique Chérifien, Série Géologie Et Géographie Physique 2:1–246

Saaty TL (1977) A scaling method for priorities in hierarchical structures. J Math Psychol 15:234–281

Saaty TL (1980) Multicriteria Decision Making. The Analytic Hierarchy Process, McGrawHill, New York

Saaty TL (1990) How to make a decision: The Analytic Hierarchy Process. Eur J Oper Res 48(1):9–26. https://doi.org/10.1016/0377-2217(90)90057-I

Taheri K, Thomas M, Missimer TM, Moayedi H, Mohseni F (2020) Critical Zone Assessments of an Alluvial Aquifer System Using the Multi-influencing Factor (MIF) and Analytical Hierarchy Process (AHP) Models in Western Iran. Nat Resources Res 29:1163–1191

Taheri K, Shahabi H, Chapi K, Shirzadi A, Gutiérrez F, Khosravi K (2019) Sinkhole susceptibility mapping: A comparison between Bayes-based machine learning algorithms 30(7):730–745. https://doi.org/10.1002/ldr.3255

Thanh LN, De Smedt F (2012) Application of an analytical hierarchical process approach for landslide susceptibility mapping in A Luoi district, Thua Thien Hue Province. Vietnam. Environ Earth Sci 66(7):1739–1752

Theilen-Willige B, Ait Malek H, Charif A, El Bchari F, Chaibi M (2014) Remote sensing and GIS contribution to the investigation of karst landscapes in NW-Morocco. Geosciences 4:50–72

Tzeng CM, Huang CC (2011) Application of the integrated model in sinkhole hazard mapping: a case study of Tainan City, Taiwan. Environ Earth Sci 64(4):1111–1121

Umar Z, Khan KS, Haris MM, Shafique M (2014) GIS-based landslide susceptibility mapping using frequency ratio and analytical hierarchy methods in Muzaffarabad district, Kashmir, Pakistan. Geomat Nat Haz Risk 5(3):247–263

Voogd H (1983) Multicriteria evaluation for urban and regional planning. Elsevier

Waltham T., Bell, F. & Culshaw M. (2005). Sinkholes and Subsidence — Karst and Cavernous Rocks in Engineering and Construction. Praxis Publishing, Springer, p 335

Whitman RV, BellG Culshaw MG (1999) Engineering and Environmental Impacts of Sinkholes and Subsidence. Thomas Telford, London

Wang Q, Li W (2017) A GIS-based comparative evaluation of analytical hierarchy process and frequency ratio models for landslide susceptibility mapping. Phys Geogr 38(4):318–337

Wang QQ, Li WP, Yan SS, Wu YL, Pei YB (2016) Gis based frequency ratio and index of entropy models to landslide susceptibility mapping (Daguan, China). Environ Earth Sci 75:780

Weisrock A, Lunski S (1987) Le karst post-pliocène de la région de Safi (Maroc atlantique). Karstologia : Revue De Karstologie Et De Spéléologie Physique 9(1):31–36. https://doi.org/10.3406/karst.1987.2155

Ying X, Zeng G-M, Chen GQ, Tang L, Wang K-L, Huang D-Y (2007) Combining AHP with GIS in synthetic evaluation of eco-environment quality — A case study of Hunan Province. China. Ecol Model 209(2):97–109. https://doi.org/10.1016/j.ecolmodel.2007.06.007

Witam O (1988) Étude stratigraphique et sédimentologique de la série mésozoïque du bassin de Safi. Thèse de 3ème cycle. Université Cadi Ayyad de Marrakech 212

Wu SZ and Wu YT (2016) Slope failure susceptibility analysis using GIS-based statistical models: a case study of the Chuoshui River basin, Taiwan. Environ Earth Sci 75(3):202

Yalcin A (2008) Gis-based landslide susceptibility mapping using analytical hierarchy process and bivariate statistics in Ardesen Author's personal copymodeling Earth Systems and Environment 1 3 (Turkey): comparisons of results and confirmations. CATENA 72(1):1–12

Yalcin A, Reis S, Aydinoglu AC, Yomralioglu T (2011) A GIS-based comparative study of frequency ratio, analytical hierarchy process, bivariate statistics and logistics regression methods for landslide susceptibility mapping in Trabzon, NE Turkey. CATENA 85(3):274–287

Yilmaz I (2009) Landslide susceptibility mapping using frequency ratio, logistic regression, artificial neural networks and their comparison: a case study from Kat landslides (Tokat—Turkey). Comput Geosci 35(6):1125–1138

Zhou W, Beck BF (2008) Management and mitigation of sinkholes on karst lands: an overview of practical applications. Environ Geol 55(4):837–851. https://doi.org/10.1007/s00254-007-1035-9

Publisher's Note Springer Nature remains neutral with regard to jurisdictional claims in published maps and institutional affiliations.

Springer Nature or its licensor (e.g. a society or other partner) holds exclusive rights to this article under a publishing agreement with the author(s) or other rightsholder(s); author self-archiving of the accepted manuscript version of this article is solely governed by the terms of such publishing agreement and applicable law.